2017

Investigation of the Thermal Performance of Sierpinski Carpet Fractal Fins in a Natural Convection Environment

Jennifer P. Shaffer
Georgia Southern University

Investigation of the Thermal Performance of Sierpinski Carpet Fractal Fins in a Natural Convection Environment

An Honors Thesis submitted in partial fulfillment of the requirements for
Honors in Mechanical Engineering

By
Jennifer Shaffer

Under the mentorship of Dr. David Calamas

ABSTRACT

This experimental investigation studies the thermal performance of the first four iterations of the Sierpinski carpet pattern in a natural convection environment. This particular fractal geometry is promising in that it increases the available surface area for heat transfer while simultaneously decreasing the mass of the system. This makes it a potentially advantageous design for fins or heat sinks, especially in aerospace applications where minimizing mass of the system is essential. The thermal performance was evaluated by comparing the efficiency, effectiveness, and effectiveness per unit mass for each fractal iteration. The results indicate that efficiency decreases with each fractal iteration while effectiveness per unit mass increases with fractal iteration. The fourth iteration fractal fin was found to be approximately 10.7% more effective, 10.2% less efficient, and 77.3% more effective per unit mass when compared to a traditional straight rectangular fin of equal height, width, and thickness (the zeroth fractal iteration). Based on the results of a view factor analysis, thermal radiation was found to comprise an average of 42.3%, 39.7%, 39.1%, 38.5%, and 34.9% of the total heat transfer for the zeroth, first, second, third, and fourth fractal iteration fins, respectively. Therefore, the contribution of thermal radiation to the total heat transfer of the system cannot be neglected in future studies using this fractal pattern.

Thesis Mentor: _____
Dr. David Calamas

Honors Director: _____
Dr. Steven Engel

May 2017

Department of Mechanical Engineering

University Honors Program

Georgia Southern University

Acknowledgements

I would like to thank my faculty adviser, Dr. David Calamas, for his patience and guidance with this thesis, as well as his essential role in developing the view factor analysis and in teaching me how to perform an experimental uncertainty analysis. Additionally, I would like to thank Stephen Zeigler, who helped me complete all the experimental trials for this thesis. The time they dedicated to this project cannot be understated, because without their help, this thesis would not have been possible.

I would also like to thank the University Honors Program and my mechanical engineering family here at Georgia Southern University for all the laughs, guidance, and knowledge they have provided me with these past four years.

Last, but certainly not least, I would like to thank my fiancé, family, and friends for their continued moral support of my crazy-busy lifestyle and the controlled chaos it entails.

Table of Contents

List of Figures

List of Tables

Nomenclature

The following nomenclature is used in this thesis:

A_b	Surface area of fin base, m^2
A_i	Surface area of fin embedded in insulation, m^2
A_s	Exposed surface area of fin, m^2
F_n	Average fin view factor
h	Average heat transfer coefficient, $W/m^2 \cdot K$
I	Current supplied, A
k	Thermal conductivity, W/m·K
m	Mass, kg
n	Fractal iteration
P	Power supplied, W
$\dot{Q}_{conv}$	Heat dissipated by convection, W
$\dot{Q}_{loss}$	Heat loss through insulation, W
$\dot{Q}_{rad}$	Heat dissipated by thermal radiation, W
t	Thickness of fin, m
T	Temperature, K
T_{amb}	Ambient temperature, K
T_{base}	Average temperature at base of fin as measured by infrared camera, K
T_s	Average surface temperature of fin (average of T_{base} and T_{tip}), K
T_{tip}	Average temperature at tip of fin as measured by infrared camera, K
V	Voltage supplied, V
w	Width of fin, m

w_s Experimental uncertainty

ε Emissivity

ε_{fin} Fin effectiveness

ε_{fin}/m Fin effectiveness per unit mass, kg^{-1}

η Fin efficiency

ρ Density, kg/m^3

σ Stefan-Boltzmann constant, 5.67×10^{-8} $W \cdot m^{-2} \cdot K^{-4}$

1. Introduction

1.1 Background and Motivation

Fins and heat sinks are normally used as a passive means to dissipate waste heat in electronic systems. This serves a critical purpose to eliminate waste heat that could otherwise cause premature failure of system components or reduce reliability. Passive thermal management strategies of electronic systems (i.e. heat sinks and fins) is preferred to active thermal management, as active thermal management systems (i.e. fans or heat pumps) have to introduce energy from an external source (usually in the form of electricity) in order to boost the rate of heat transfer from the system. Passive thermal management strategies do not require electricity to operate and are generally less complex and more cost-effective to implement than active thermal management systems. The use of finned heat sinks is one of the most common passive thermal management technique of electronic systems and utilizes natural convection as the primary method for heat dissipation.

In most applications, using a lesser amount of volume of material is desirable to keep costs low, though this is often a challenge as convective heat transfer is directly proportional to the amount of surface area available. The appeal of certain fractal geometries is their ability to increase the amount of available surface area while simultaneously decreasing the volume and mass of the system. In certain industries, such as the aerospace industry where the cost to access space is substantial, the significant cost savings resulting from the mass reduction of a system may justify the cost of additional manufacturing to fabricate fractal fins for passive thermal management of electrical systems. For example, NASA reports that the cost to put one pound of payload into low

earth orbit is approximately $10,000 ($22,000 per kilogram) [1]. Recent developments by private aerospace companies have lowered the estimated cost of sending future payloads into low earth orbit to approximately $2,000-$3,000 per kilogram, although sending future materials to the further reaches of space will continue to be relatively expensive [2].

1.2 Objectives

The primary objectives of this investigation is to experimentally determine the performance of the first four fractal iterations of the Sierpinski carpet pattern fins using the two most common fin performance metrics, fin efficiency and fin effectiveness. The effectiveness per unit mass will be studied as an additional performance metric of interest. The results of this study will be compared to an earlier, similar study to study the scalability of these results to fins of different scale.

This research expands on previous research [3] [4] [5] by experimentally studying the thermal performance the first four iterations of the Sierpinski carpet pattern fins on a smaller scale to examine the scalability of results between fin scales. The previously tested large-scale Sierpinski carpet fractal fin dimensions were 4” by 4” by 1/8”, whereas the small-scale Sierpinski carpet fractal fin dimensions for this experiment were 2” by 2” by 1/16”. The width-to-thickness ratio of the fins of either scale is 32. An estimation of the contribution of thermal radiation heat transfer to the total heat dissipated from the smaller fins was also taken into account to support the theory that the heat loss due to thermal radiation is not insignificant.

1.3 Sierpinski Carpet Pattern Fractal Fins

Fractal patterns are defined as repeating instances of similar patterns at progressively smaller scales. The Sierpinski carpet pattern subdivides itself into nine equal squares and removes the center square from each iteration. This technique of subdivision and removal is then applied recursively to the eight remaining sub-squares, *ad infinitum*. The Sierpinski carpet pattern was selected for this fin design due to its unique ability to decrease mass of the fin while increasing the surface area available for heat transfer on the fin. The first four fractal iterations of the Sierpinski carpet pattern fins are shown below in Figure 1.

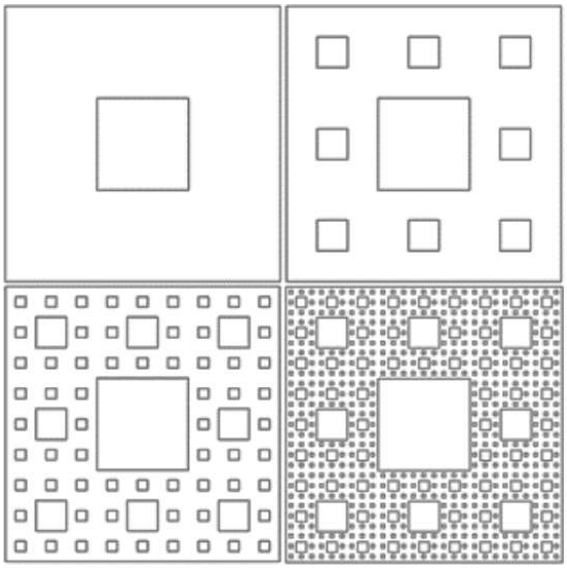

Figure 1. First Four Iterations of Sierpinski Carpet Pattern Fractal Fins

The mass of any Sierpinski carpet pattern fin is only dependent on fractal iteration and can be calculated using Eq. (1) below.

$$m(n) = \left[w^2 - \sum_{1}^{n} 8^{n-1} \left(\frac{w}{3^n}\right)^2 \right] \rho t \tag{1}$$

The surface area of any Sierpinski carpet pattern fin is also dependent on fractal iteration and can be calculated using Eq. (2) below.

$$A_s(n) = 2w^2 + 3wt - \sum_{1}^{n} 8^{n-1}\left[2\left(\frac{w}{3^n}\right)^2 - 4\left(\frac{w}{3^n}\right)t\right] \quad (2)$$

Additional material is removed with each fractal iteration, resulting in a mass reduction for each increasing iteration, as shown in Figure 2 below.

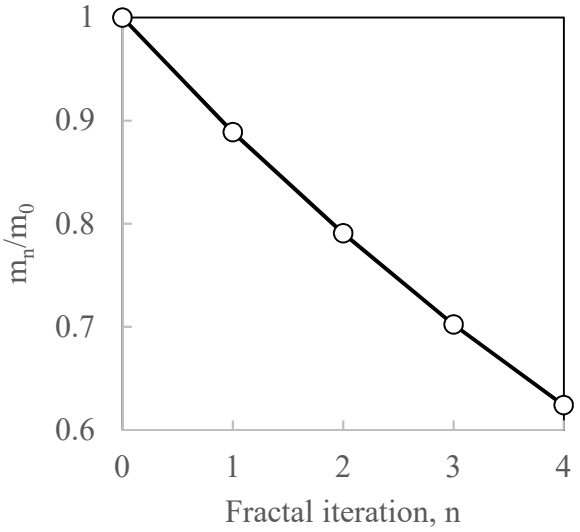

Figure 2. Ratio of Fin Mass as a Function of Fractal Iteration

While mass is dependent only on fractal iteration, the surface area of the Sierpinski carpet fractal fins is also dependent on the width-to-thickness ratio of the fin. The width-to-thickness ratio of the fins used in this experiment is 32 (2" width, 1/16" thickness). The ratio of surface areas for each fractal iteration compared to the 0^{th} (baseline) fin as a function of fractal iteration is given below in Figure 3.

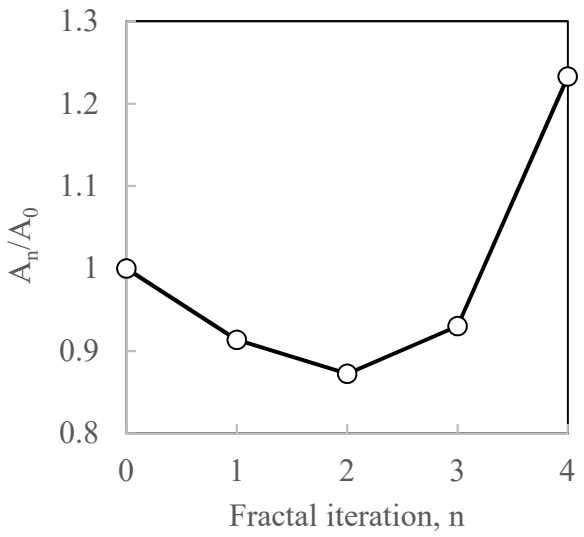

Figure 3. Ratio of Fin Iteration Surface Area as Function of Fractal Iteration

1.4 Literature Review

The primary purpose of heat sinks in electrical systems is to passively dissipate excess heat from the systems to avoid premature failure of components and optimize performance. The goal of any heat sink is to dissipate heat effectively enough to keep the temperature within the operational limits of the device.

As heat transfer due to natural convection is directly proportional to the exposed surface area of a fin or other extended surface, fractal geometries are being studied for their ability to increase available surface area while reducing mass with each fractal iteration. This reduction in mass is highly sought after in several applications, specifically in the design of heat transfer components where maximized heat transfer with minimal mass of material is ideal, such as spacecraft thermal management [6]. In previous experiments, the increase in surface area per fin volume that a fractal design provides resulted in a higher overall fin effectiveness [5] [7].

Problems are typically encountered when trying to scale performance of these fractal designs from the microscale (where most are studied) to meso- and macro-scale applications. Thus far, hierarchical designs involving fractal networks commonly found in nature have proven effective in solving the scaling dilemma [7]. In a previous study conducted by Calamas and Baker [8], it was found that the microscale tree-like branching fin had the highest effectiveness and efficiency when compared to the mesoscale and macroscale fins of the same design in a natural convection environment. However, natural convective and radiant heat transfer behavior of fractal fins at different scales has not been thoroughly researched at this point, and so this research aims in part to examine the scalability of fin performance of the Sierpinski carpet pattern fractal fins.

Additionally, previous researchers have tended to focus solely on natural convection as the primary mode of heat transfer, neglecting the heat loss due to radiation [6]. This seems to be a grossly false assumption, as noted first by Azarkish. Azarkish studied the optimization of longitudinal fins that volumetrically generated heat and found that even for small values of surface emissivity, the contribution of thermal radiation to the overall heat transfer rate was large relative to the other forms of heat transfer and should not be neglected [9].

There were also several studies by Shaeri and several other researchers that investigated the thermal performance of various non-traditional, non-fractal fin geometries that incorporated perforations to enhance heat transfer in both natural and forced convection environments. Shaeri conducted several computational studies of heat sinks that incorporated straight rectangular fins with varying perforation sizes and porosity in forced convection environments with laminar flow ($100<Re_D<350$) and found

that fins with higher porosity (more perforations) performed better than non-perforated fins with regards to effectiveness and effectiveness per unit mass [10], a finding that was later supported by another study in which he studied the fin effectiveness of perforated fins in a forced convection environment with calculated Reynolds numbers between 2000 and 5000 [11]. Shaeri then investigated the effect of perforation sizes on the effectiveness of the fins and found that the perforations in the fins had no effect on the total drag of the fin, although perforated fins did experience a higher friction drag and lower pressure drag than the solid fins [12].

Also investigating non-traditional, non-fractal fin geometries for effectiveness, Yu experimentally and computationally studied the performance of a radial heat sink both with and without thermal radiation in a natural convection environment. By varying the emissivity of the heat sink, Yu et al. determined that thermal radiation could account for up to 27% of the total heat transfer rate of the system [13]. His conclusion that neglecting thermal radiation in optimizing a fin design could result in a less-than-optimal fin configuration, and this finding was later supported by Calamas et al., who tested the thermal performance of larger-scale Sierpinski carpet pattern fractal fins in a natural convection environment and found that thermal radiation could account for 30-40% of the overall heat transfer rate of the system [3].

Initially, Dannelley and Baker first studied certain fractal geometries such as the modified Koch snowflake and the Sierpinski carpet pattern to improve the thermal performance of fins for passive thermal management. They concluded that the effectiveness of fractal fins was directly proportional to the amount of surface area available for heat transfer [6]. Dannelley and Baker tested the first three fractal iterations

of each pattern and isolated heat transfer by natural convection in their calculations and did not consider the contribution of thermal radiation to the overall heat transfer rate of the system. They could not experimentally test the fourth iteration due to fabrication constraints, although they did test the fourth iteration in a computational model and found that effectiveness and effectiveness per unit mass improved compared to the zeroth iteration (baseline fin) [5]. Dannelley and Baker also studied various width-to-thickness ratios with the Sierpinski carpet pattern fractal fins and found that fin effectiveness was inversely proportional to the width-to-thickness ratio of the fins.

Computational studies on the use of fractal geometries to enhance the performance of fins by dissipate waste heat through thermal radiation to free space were also conducted by Dannelley and Baker, and they found that despite decreases in fin efficiency and fin effectiveness for the first three fractal iterations of the Sierpinski carpet pattern, the fin effectiveness per unit mass still increased for each fractal iteration [14]. In doing so, they also developed a correlation for the effectiveness of such fins radiating to free space for any surface emissivity greater than or equal to 0.8.

Most recently, Calamas et al. experimentally studied the thermal performance of the first four iterations of large-scale Sierpinski carpet pattern fractal fins in a natural convection environment, and his results supported Dannelley and Baker's hypothesis that the fourth fractal iteration fin performed with a higher fin effectiveness and effectiveness per unit mass than the zeroth iteration (baseline) fin [3] , [6]. Keten continued the study of the large-scale Sierpinski carpet pattern fractal fins in both natural and forced convection environments, and his results supported the hypothesis that the fin effectiveness and effectiveness per unit mass increases relative to the zeroth iteration

(baseline) fin starting with the fourth iteration fin [5]. This experimental investigation follows a procedure similar to those established by Calamas et al. and Keten to test the fins in a natural convection environment while also accounting for the heat loss due to thermal radiation, and one of the objectives of this study is to compare the results of the thermal performance of the small-scale Sierpinski carpet pattern fractal fins to the larger-scale fractal fins tested by Keten. It is important to note that while a view factor analysis was performed for this study to calculate the amount of radiation that escaped to the surrounding for the fins with smaller perforation, no such study existed at the time of Keten's study, and therefore this has to be taken into consideration when results must be compared between studies.

2. Experimental Methodology

The first four iterations of the fractal fins and the base pattern used in the experimental trials can be seen below in Figure 4.

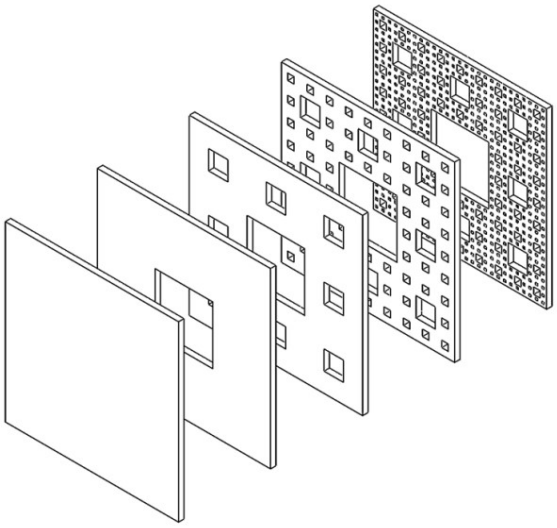

Figure 4. Base (0th) Fin and First Four Fractal Iterations of Sierpinski Carpet Pattern Fins [5]

The width and height of each square fin was 2 inches (5.08cm), and each fin had a thickness of 1/16 inch (0.16cm). The width-to-thickness ratio of these fins was 32. The fins were fabricated out of aluminum 5052 and anodized with a matte black surface finish to approximate a surface emissivity (ε) of 0.99. The mass and surface area for each small fin is given below in Table 1. These values were calculated using Eq. (1) and Eq. (2) and the dimensions and masses were experimentally verified with a digital micrometer and a scale, respectively.

Table 1. Small-Scale Sierpinski Carpet Fin Masses and Surface Areas

n	A_s (cm^2)	m (g)
0	54.03	10.98
1	49.37	9.76
2	47.14	8.68
3	50.26	7.71
4	66.62	6.85

Kapton® flexible thin film insulated heaters were adhered to the base of each fin using a pressure-sensitive adhesive (Omega® KHLV-104/2-P) to supply a known heat transfer rate to the base of each fin, which were then encased in Techlite® melamine foam insulation (k = 0.036 W/m·K) to minimize heat loss. Additional melamine foam insulation was placed under the experimental setup as a precautionary measure. The power supplied to the thin film heaters was controlled by an adjustable power supply (B&K Precision 9130). An Omega® T-type probe thermocouple was used to measure the ambient temperature in the laboratory, while an Omega® T-type surface thermocouple was used to measure the surface temperature of the flexible thin film heaters at the base of the fins during the experiments.

Additional T-type probe thermocouples were used to measure heat loss through the insulation at three different locations around the fin: ½ inch (1.27cm) from the back of the fin, ½ inch (1.27cm) from the side of the fin, and ½ inch (1.27cm) below the fin. A benchtop temperature controller (Omega MCS-2110) was used to monitor the temperature of the thin film heaters to ensure that the thin film heaters did not exceed the safe operating temperature range of the melamine foam insulation. A 16-channel thermocouple compact data acquisition (DAQ) module (National Instruments 9213) was used with National Instruments LabVIEW software to monitor and record the temperatures of all thermocouples during experimental trials. Final temperatures were recorded after each thermocouple reached steady-state.

To watch the real-time temperature profiles along the fractal fin surface, a FLIR® A325sc infrared camera and its accompanying ResearchIR software was implemented, and the average steady-state temperatures along the tip and base of the fins were recorded using this software at the ended of each experimental trial. A diagram of the complete experimental setup is given below in Figure 5.

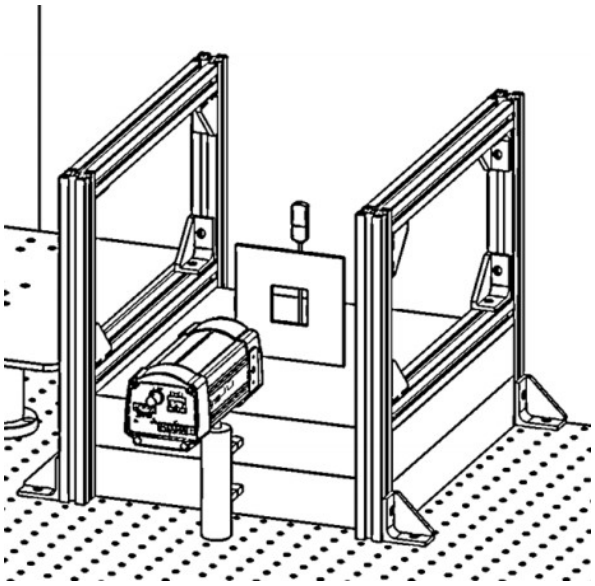

Figure 5. Experimental Setup

A total of 75 trials were conducted, as each fractal fin iteration and baseline fin were tested five times at each power input level (2.5W, 5W, and 10W). Trials using a power input above 10W were unsafe to conduct with the current experimental setup, as the temperature of the thin film heaters would exceed the safe operating temperature of the melamine foam insulation (approximately 176°C) and present a melting/flash fire hazard. Each experimental trial lasted between 20-35 minutes to reach steady-state values across all thermocouple readings, as trials with higher power inputs required less time to reach steady-state values than trials with lower power inputs.

3. Data / Calculations

3.1 Data

Each iteration of the Sierpinski carpet pattern fractal fins was subjected to three levels of power input (2.5W, 5W, and 10W) with five trials each, resulting in a total of 75 experimental trials.

3.2 Experimental Calculations

The total power supplied to each fractal fin via the flexible thin film heaters was calculating using a variation of Ohm's law, as shown below in Eq. (3).

$$P = IV \tag{3}$$

The heat loss through the melamine foam insulation was calculated using Fourier's law and the temperatures measured by the T-type thermocouples placed ½ inch (1.27cm) behind, beside, and below the fin, as shown below in Eq. (4).

$$\dot{Q}_{loss} = \sum -kA_i \frac{\partial T}{\partial n} \tag{4}$$

After a view factor analysis of the fins to estimate the amount of radiation lost to the surroundings, it was found that a view factor of one could not be assumed for all fin iterations, as not all heat was radiated to the surroundings. The amount of heat radiated to the surroundings depended on a variety of factors, including perforation size, number of perforations, and width-to-thickness ratio of the fins compared to the dimensions of the perforation. An average fin view factor was computed for each iteration based on these parameters, and the calculated average fin view factors are summarized in Table 2 below.

Table 2. Average Fin View Factors

n	Average Fin View Factor (F_n)
0	1.000
1	0.9972
2	0.9797
3	0.8966
4	0.6737

This analysis was particularly relevant for radiation calculations concerning the fourth fractal iteration, as the average fin view factor suggests that only 67.4% of the radiation from the fin escapes to the surroundings and contributes to the overall heat dissipation of the fin, while the remaining 32.6% of the radiation becomes engaged in inter-surface thermal radiation within the ever-smaller fin perforations. This trend in decreasing average fin view factors with respect to fractal iteration is expected to continue in the later iteration fractal fins, with a higher percentage of the radiated heat failing to escape to the surroundings and instead engaging in inter-surface thermal radiation.

Using the average fin view factors, the heat dissipated due to thermal radiation was calculated using the ambient temperature and the average surface temperature of the fin as well as the respective average fin view factor, using Eq. (5) below.

$$\dot{Q}_{rad} = \varepsilon\sigma F_n A_s \left(T_s^4 - T_{amb}^4\right) \tag{5}$$

The rate of heat transfer due to convection was then calculated using Eq. (6) below.

$$\dot{Q}_{conv} = P - \dot{Q}_{loss} - \dot{Q}_{rad} \tag{6}$$

Next, the average heat transfer coefficient was calculated using Eq. (7) below.

$$h = \frac{\dot{Q}_{conv}}{A_s(T_s - T_{amb})} \tag{7}$$

When evaluating the performance of fins, the two most common performance metrics are fin efficiency and fin effectiveness. Fin efficiency is calculated as the ratio of the actual heat transfer achieved by the fin to the ideal heat transfer from the fin. The ideal heat transfer rate comes from assuming that the entire fin is uniformly at the base temperature, which means that the fin would have infinite conductivity. The fin efficiency can be calculated using Eq. (8) below.

$$\eta = \frac{\dot{Q}_{conv}}{hA_s(T_{base} - T_{amb})} \tag{8}$$

On the other hand, fin effectiveness compares the amount of heat transfer achieved by the fin to the amount of heat transfer that would occur without a fin in that same area. Fin effectiveness is therefore calculated as the ratio of the actual heat transfer rate achieved by the fin to the heat transfer rate of the base area of the fin, and can be calculated using Eq. (9) below.

$$\varepsilon_{fin} = \frac{\dot{Q}_{conv}}{hA_b(T_{base} - T_{amb})} \tag{9}$$

4. Results

4.1 Initial Results

A summary of the results for each trial at each power input is given below in Table 3. A summary of the average results for each iteration at each power input will be discussed in the statistical analysis section of this thesis.

Table 3. Fin Performance Metrics for All Trials

Power Input	2.5W			5W			10W		
Iteration	η	ε	ε/m_n (kg^{-1})	η	ε	ε/m_n (kg^{-1})	η	ε	ε/m_n (kg^{-1})
0	0.92	61.84	5632.42	0.92	61.35	5587.38	0.91	61.15	5569.14
	0.92	61.86	5633.81	0.92	61.35	5587.90	0.92	61.43	5594.96
	0.93	62.04	5650.62	0.92	61.34	5587.08	0.92	61.39	5591.17
	0.93	62.01	5648.21	0.91	61.20	5574.48	0.92	61.42	5594.09
	0.93	62.13	5658.83	0.92	61.38	5590.15	0.92	61.38	5590.44
1	0.91	55.92	5730.28	0.91	55.57	5694.46	0.90	55.13	5648.95
	0.91	55.78	5715.33	0.90	55.17	5652.83	0.90	55.01	5636.33
	0.90	55.32	5668.49	0.90	55.19	5655.21	0.90	54.92	5627.66
	0.91	55.83	5721.04	0.91	55.41	5677.71	0.90	55.13	5649.06
	0.91	55.73	5710.20	0.91	55.49	5685.82	0.90	55.09	5645.19
2	0.90	52.67	6071.92	0.89	51.89	5981.11	0.89	51.92	5985.29
	0.91	52.91	6098.64	0.89	51.99	5992.83	0.89	51.86	5977.56
	0.90	52.74	6079.01	0.89	52.14	6009.86	0.89	51.74	5964.32
	0.90	52.48	6049.50	0.90	52.86	6092.93	0.88	51.51	5937.92
	0.90	52.35	6034.38	0.91	53.10	6120.52	0.88	51.59	5946.48
3	0.88	55.10	7145.51	0.88	54.77	7102.44	0.86	53.36	6920.46
	0.89	55.19	7157.73	0.88	54.57	7077.06	0.87	53.95	6996.11
	0.88	54.78	7104.43	0.88	54.71	7095.13	0.87	53.95	6995.97
	0.88	54.93	7123.78	0.86	53.89	6989.04	0.86	53.64	6956.60
	0.89	55.18	7156.52	0.88	54.61	7082.03	0.86	53.67	6960.67
4	0.82	68.00	9921.17	0.83	68.69	10021.77	0.82	67.60	9862.92
	0.83	68.64	10014.76	0.82	67.48	9844.74	0.83	68.18	9946.48
	0.83	68.89	10050.83	0.82	67.64	9868.03	0.82	67.67	9872.91
	0.83	68.59	10007.29	0.83	68.21	9950.78	0.82	67.89	9905.35
	0.83	68.87	10048.20	0.82	67.53	9852.00	0.81	67.15	9796.04

To visualize trends with increasing fractal iteration, the following graphs tracking the various fin performance metrics were generated. Figure 6 below shows fin efficiency as a function of fractal iteration and power input.

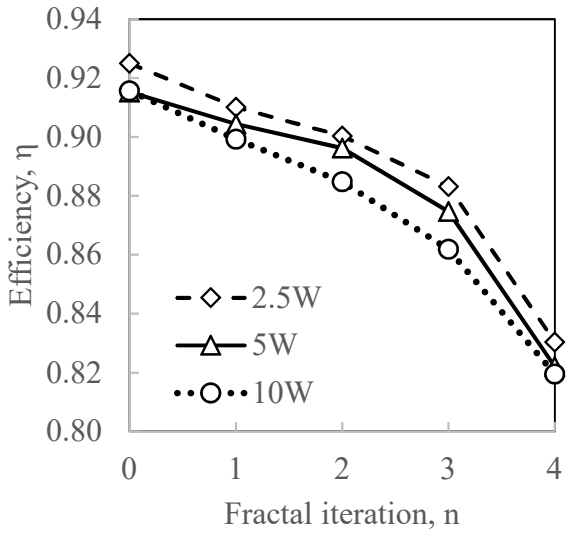

Figure 6. Fin Efficiency as a Function of Fractal Iteration and Power Input

Fin efficiency decreased steadily with each fractal iteration of the Sierpinski carpet pattern, though the fourth iteration fin only experienced a 10.2% decrease in efficiency compared to the baseline (zeroth iteration) fin.

Figure 7 below shows fin effectiveness as a function of fractal iteration and power input.

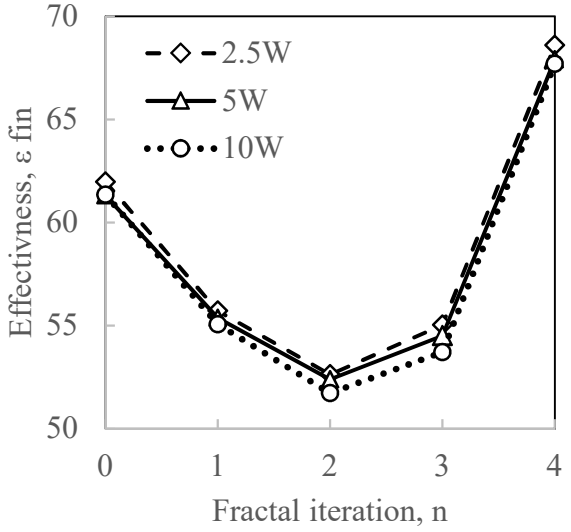

Figure 7. Fin Effectiveness as a Function of Fractal Iteration and Power Input

Up until the third iteration fin, the fin effectiveness decreased relative to the baseline fin with each fractal iteration; however, starting with the fourth iteration, the fin effectiveness begins to increase relative to the baseline fin. While the third iteration experienced an 11-12% decrease in effectiveness relative to the baseline fin, the fourth iteration experienced an increase in effectiveness of 10-11% relative to the baseline fin. This was expected, as the fin effectiveness is directly related to the exposed surface area of the fin, and the available surface area initially decreases relative to the baseline iteration until the third iteration, at which point it increases relative to the baseline iteration for the fourth iteration. For reference, the fourth iteration fin has approximately 23.3% more surface area available for convective heat transfer than the baseline iteration, whereas the second and third iteration fins have 12.8% less and 7.0% less exposed surface area than the baseline iteration, respectively. Figure 8 below shows fin effectiveness per unit mass as a function of fractal iteration and power input.

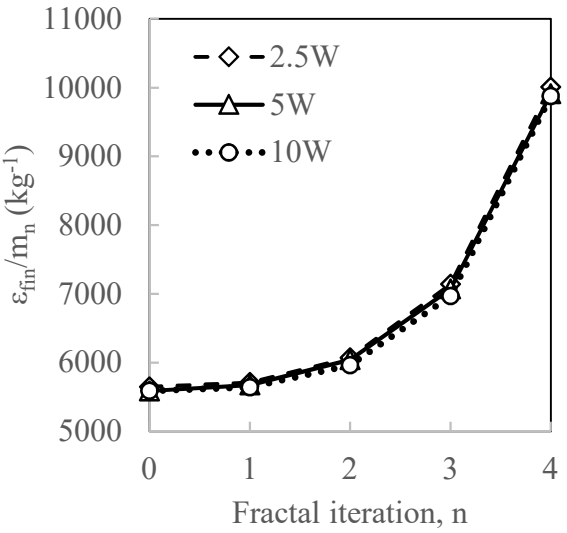

Figure 8. Fin Effectiveness per Unit Mass as a Function of Fractal Iteration and Power Input

The results suggest that the fin effectiveness per unit mass increases with each fractal iteration of the Sierpinski carpet pattern. This trend was expected, as the mass decreased exponentially with each fractal iteration of the fractal fins. For example, the fourth iteration fin experienced a 23.3% increase in exposed surface area with a 37.6% decrease in mass relative to the baseline fin.

Another focus of this research endeavor was to study the percentage of the total heat transfer of the system achieved by thermal radiation to see if it accounted for a significant portion of the heat transfer from the system. The results of the analysis calculating the approximate percent of the total heat transfer of the system due to heat loss through the insulation, dissipation by thermal radiation, and dissipation by natural convection are given below in Table 4.

It is important to note that the amount of heat loss through the insulation was approximated for the worst-case scenario in the above calculations, as the heat loss through the insulation around the fin base was assumed to be perfectly uniform and symmetrical, as shown in Figure 9 below.

These assumptions simplified the calculations to a necessary degree due to limitations of the experimental setup; however, these assumptions result in an overestimate of the heat loss through insulation, as the simplified profile assumes more heat loss through the insulation than the theoretical (actual) profile. Despite this, the heat loss through the insulation still only accounts for 10% or less of the total heat transfer of the system for each iteration. This means that the percentage of heat transfer by thermal radiation and natural convection may be slightly underestimated.

Table 4. Percent of Total Heat Transfer of System with Respect to Thermal Radiation and Natural Convection for All Power Inputs and Iterations

Power Input	n	Percent of Total Heat Transfer of System Attributed to…		
		Heat loss through insulation	Dissipation by Thermal Radiation	Dissipation by Natural Convection
2.5W	0	8.2%	42.2%	49.7%
	1	8.6%	39.3%	52.1%
	2	7.4%	39.7%	52.9%
	3	10.3%	37.7%	51.9%
	4	10.3%	34.5%	55.1%
5W	0	7.2%	41.3%	51.5%
	1	7.8%	38.8%	53.4%
	2	7.2%	36.9%	56.0%
	3	9.1%	37.0%	53.9%
	4	9.3%	33.7%	57.0%
10W	0	6.2%	43.3%	50.5%
	1	6.7%	41.0%	52.3%
	2	6.0%	39.6%	54.5%
	3	8.0%	40.8%	51.1%
	4	8.2%	36.5%	55.3%

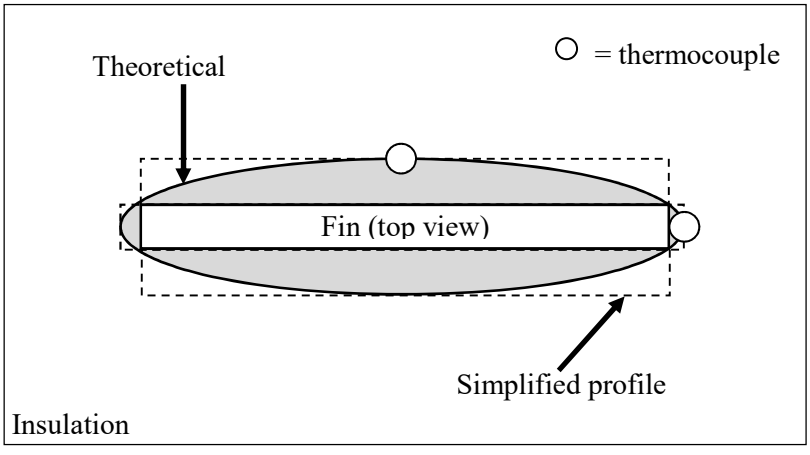

Figure 9. Theoretical vs. Simplified Heat Conduction Profiles (Top View)

To examine the trends of heat dissipation, the average heat transfer contributions from both radiation and natural convection were calculated and expressed as a percentage of the total heat transfer of the system. To visualize the different percentages of overall heat dissipation due to radiation versus natural convection for each fractal iteration, the results of the calculations were graphed in Figure 10, Figure 11, and Figure 12 below.

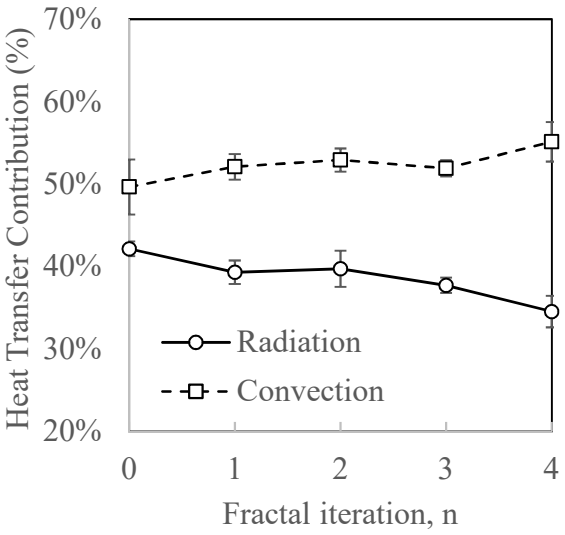

Figure 10. Average Percentages of Heat Transfer Contributions, 2.5W Trials

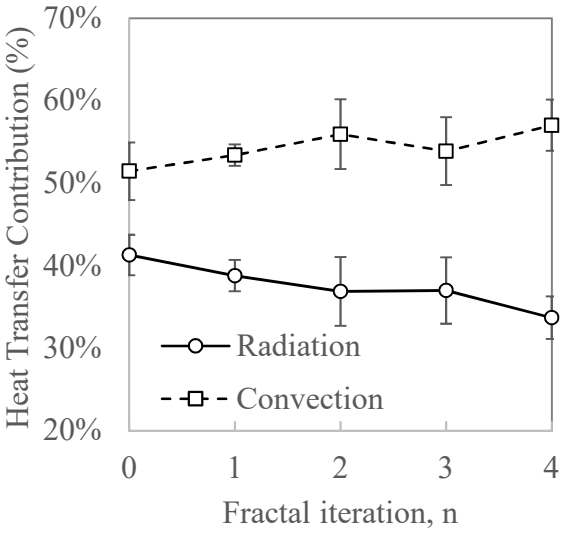

Figure 11. Average Percentages of Heat Transfer Contributions, 5W Trials

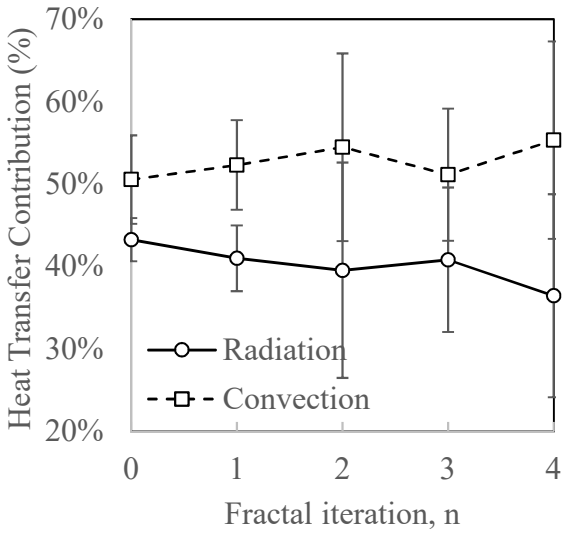

Figure 12. Average Percentages of Heat Transfer Contributions, 10W Trials

From the figures above, although radiation constitutes a significant percentage of the overall heat transfer of the system (between 33-42%), natural convection clearly remains the dominant mode of heat transfer at all power levels for each iteration. It may also be relevant to note that there is a noticeable, although slight, decrease in the percentage of overall heat transfer by radiation for the 4^{th} iteration as compared to the other iterations. This was expected due to the application of the average fin view factor in the calculations, as it was found during the view factor analysis that while between 90-100% of the radiation escapes into the surrounding atmosphere for the zeroth through third fractal iterations, only approximately 67.4% of the heat radiated by the fourth iteration fin escaped to the surroundings, whereas the other 32.6% of the radiated heat remained trapped in the ever-smaller fin perforations. Regardless, it is clear from the analysis above that thermal radiation accounts for a significant portion of the total heat transfer of the system (between 33-42%), and therefore the contributions of thermal radiation cannot be neglected in future investigations.

4.2 Statistical Analysis

To better understand the general trends across fractal fin iterations, a statistical analysis of the initial results for each fin performance metric at each power level was performed, and the results are tabulated below in Table 5.

Table 5. Average Fin Performance Metrics for Various Power Inputs

Power Input	n	η		ε_{fin}		ε_{fin}/m_n (kg^{-1})	
		Avg.	Std.	Avg.	Std.	Avg.	Std.
2.5W	0	0.93	0.002	61.98	0.12	5644.78	11.36
	1	0.91	0.004	55.72	0.23	5709.07	23.88
	2	0.90	0.004	52.63	0.22	6066.69	25.20
	3	0.88	0.003	55.04	0.18	7137.60	23.00
	4	0.83	0.004	68.60	0.36	10008.45	52.52
5W	0	0.92	0.001	61.32	0.07	5585.40	6.22
	1	0.90	0.003	55.37	0.18	5673.21	18.51
	2	0.90	0.009	52.39	0.55	6039.45	63.02
	3	0.87	0.006	54.51	0.35	7069.14	45.91
	4	0.82	0.006	67.91	0.53	9907.46	76.66
10W	0	0.92	0.002	61.35	0.12	5587.96	10.69
	1	0.90	0.001	55.06	0.09	5641.44	9.28
	2	0.88	0.003	51.72	0.17	5962.31	20.06
	3	0.86	0.004	53.72	0.24	6965.96	31.61
	4	0.82	0.005	67.70	0.38	9876.74	55.68

To compare the average fin performance metrics to those of the baseline fins, the percent changes of the average performance metrics of each iteration relative to the baseline iteration were calculated, and the results are given below in Table 6. The fourth iteration experienced an average 10.2% decrease in efficiency while experiencing a

simultaneous 10.7% increase in effectiveness and 77.3% increase in effectiveness per unit mass relative to the baseline fin. This suggests that it would be an improved design compared to the baseline fin (a traditional, solid, straight rectangular fin) for passive heat dissipation of electronic systems. However, the additional cost to manufacture a fourth iteration fin of this fractal design would need to be taken into consideration when justifying this design for a typical heat sink application.

Table 6. Percent Change of Average Performance Metrics Relative to Baseline Fin

Power Input	n	η		ε_{fin}		ε_{fin}/m_n (kg^{-1})	
		Avg.	*Percent Change from 0th Iteration*	*Avg.*	*Percent Change from 0th Iteration*	*Avg.*	*Percent Change from 0th Iteration*
2.5W	0	0.93	0.0%	61.98	0.0%	5644.78	0.0%
	1	0.91	-1.6%	55.72	-10.1%	5709.07	1.1%
	2	0.90	-2.7%	52.63	-15.1%	6066.69	7.5%
	3	0.88	-4.5%	55.04	-11.2%	7137.60	26.4%
	4	0.83	-10.2%	68.60	10.7%	10008.45	77.3%
5W	0	0.92	0.0%	61.32	0.0%	5585.40	0.0%
	1	0.90	-1.2%	55.37	-9.7%	5673.21	1.6%
	2	0.90	-2.1%	52.39	-14.6%	6039.45	8.1%
	3	0.87	-4.4%	54.51	-11.1%	7069.14	26.6%
	4	0.82	-10.2%	67.91	10.7%	9907.46	77.4%
10W	0	0.92	0.0%	61.35	0.0%	5587.96	0.0%
	1	0.90	-1.8%	55.06	-10.3%	5641.44	1.0%
	2	0.88	-3.4%	51.72	-15.7%	5962.31	6.7%
	3	0.86	-5.9%	53.72	-12.4%	6965.96	24.7%
	4	0.82	-10.5%	67.70	10.3%	9876.74	76.8%

The fourth iteration experienced an average 10.2% decrease in efficiency while experiencing a simultaneous 10.7% increase in effectiveness and 77.3% increase in effectiveness per unit mass relative to the baseline fin. This suggests that it would be an improved design compared to the baseline fin (a traditional, solid, straight rectangular fin) for passive heat dissipation of electronic systems. However, the additional cost to manufacture a fourth iteration fin of this fractal design would need to be taken into consideration when justifying this design for a typical heat sink application.

4.3 Experimental Uncertainty Analysis

Experimental uncertainty calculations were carried out per the root of the sum of the squares (RSS) method presented by Wheeler and Ghanji, as shown in Eq. (10) below.

$$w_s = \left[\sum \left\{\left(\frac{\partial S}{\partial x_n}\right) w_{x_n}\right\}^2\right]^{1/2} \tag{10}$$

This was done to demonstrate the "propagation of uncertainty" due to the various measurement tools and techniques used in the experimental methodology [15]. The measurement uncertainties for each piece of measuring equipment used to collect data are given in Table 7 below to a 95% confidence level. These values were used in the calculation of the experimental uncertainty values.

Table 7. List of Measurement Uncertainties for Uncertainty Analysis

Measurement/Equipment	Uncertainty
T-type thermocouples	1°C
FLIR infrared camera	2°C
Voltage output from power supply	0.01% + 3mV
Current output from power supply	0.1% + 3mA
Digital micrometer (fin dimensions)	0.01mm
Scale (fin mass)	0.1g

Additionally, several key assumptions made during the experimental uncertainty analysis included the following:

1. All properties (i.e. thermal conductivity, the dynamic viscosity, etc.) were assumed to be constant with zero uncertainty.
2. All length terms (i.e. length, width, height, thickness, etc.) and therefore all area terms (i.e. base area, surface area, etc.) were assumed to have zero uncertainty. This is because these values did not change between trials.
3. The mass of the fins was assumed to have an uncertainty of zero, as the mass did not vary between trials of the same fin.

Using these key assumptions to nullify terms with an assumed uncertainty of zero, the experimental uncertainty of the fin efficiency was calculated using the simplified Eq. (11) below.

$$w_\eta = \left[\left(\frac{\partial \eta}{\partial \dot{Q}_{conv}} w_{\dot{Q}_{conv}}\right)^2 + \left(\frac{\partial \eta}{\partial h} w_h\right)^2 + \left(\frac{\partial \eta}{\partial T_{base}} w_{T_{base}}\right)^2 + \left(\frac{\partial \eta}{\partial T_{amb}} w_{T_{amb}}\right)^2\right]^{\frac{1}{2}}$$

$$= \left[\left(\frac{1}{hA_s(T_{base} - T_{amb})} w_{\dot{Q}_{conv}}\right)^2 + \left(-\frac{\dot{Q}_{conv}}{h^2 A_s(T_{base} - T_{amb})} w_h\right)^2 \right. \quad (11)$$

$$\left. + \left(-\frac{\dot{Q}_{conv}}{hA_s(T_{base} - T_{amb})^2} w_{T_{base}}\right)^2 + \left(\frac{\dot{Q}_{conv}}{hA_s(T_{base} - T_{amb})^2} w_{T_{amb}}\right)^2\right]^{\frac{1}{2}}$$

Similarly, the experimental uncertainty of the fin effectiveness was calculated using the simplified Eq. (12) below.

$$w_{\varepsilon_{fin}} = \left[\left(\frac{\partial \varepsilon_{fin}}{\partial \dot{Q}_{conv}} w_{\dot{Q}_{conv}}\right)^2 + \left(\frac{\partial \varepsilon_{fin}}{\partial h} w_h\right)^2 + \left(\frac{\partial \varepsilon_{fin}}{\partial T_{base}} w_{T_{base}}\right)^2 + \left(\frac{\partial \varepsilon_{fin}}{\partial T_{amb}} w_{T_{amb}}\right)^2\right]^{\frac{1}{2}}$$

$$= \left[\left(\frac{1}{hA_b(T_{base} - T_{amb})} w_{\dot{Q}_{conv}}\right)^2 + \left(-\frac{\dot{Q}_{con}}{h^2 A_b(T_{base} - T_{amb})} w_h\right)^2 \right. \quad (12)$$

$$\left. + \left(-\frac{\dot{Q}_{conv}}{hA_b(T_{base} - T_{amb})^2} w_{T_{base}}\right)^2 + \left(\frac{\dot{Q}_{conv}}{hA_b(T_{base} - T_{amb})^2} w_{T_{amb}}\right)^2\right]^{\frac{1}{2}}$$

Lastly, the experimental uncertainty of the fin effectiveness per unit mass was calculated using the simplified Eq. (13) below.

$$w_{\varepsilon_{fin}/m} = \left[\left(\frac{\partial \varepsilon_{fin}/m}{\partial \varepsilon_{fin}} w_{\varepsilon_{fin}}\right)^2\right]^{\frac{1}{2}} = \left[\left(\frac{1}{m} w_{\varepsilon_{fin}}\right)^2\right]^{\frac{1}{2}} \quad (13)$$

The calculated experimental uncertainty values for all input power levels based on the above measurement uncertainties are given below in Table 8.

Table 8. Experimental Uncertainty for Various Power Inputs

Power Input	n	w_η	w_ε	$w_{\varepsilon/m}$ (kg^{-1})
2.5W	0	0.102	6.86	625.00
	1	0.086	5.73	522.20
	2	0.076	5.11	465.69
	3	0.083	5.55	505.69
	4	0.118	7.89	718.43
5W	0	0.061	4.10	373.54
	1	0.052	3.46	315.47
	2	0.046	3.10	282.77
	3	0.050	3.34	304.29
	4	0.070	4.69	427.14
10W	0	0.041	2.72	247.66
	1	0.034	2.29	208.14
	2	0.030	2.03	184.66
	3	0.034	2.27	207.09
	4	0.046	3.11	282.94

5. Discussion

While fin efficiency and effectiveness are both important fin performance metrics, the primary draw of the Sierpinski carpet pattern as a potential fin is its ability to reduce mass while increasing surface area available for heat transfer, which is desirable in applications where reduction in mass while maintaining or improving effectiveness of the fin is sought after. Essentially, the Sierpinski carpet pattern fractal fin is able to achieve higher performance on a per unit mass basis. Consequently, the effectiveness per unit mass of the fin was considered to be a more important fin performance metric.

When examining the trends across all power inputs, the efficiency of the fins steadily decreased with each fractal iteration, and the fourth iterations were found to be 10.2% less efficient than the baseline iteration and was the least efficient fin design

tested. One reason for the decreased efficiency of each successive iteration was the increased temperature gradient between the base and tip of the fin with each iteration, caused in part by the presence of an increased number of perforations in the fins.

Additionally, the fourth iteration was the only fin tested that was found to be 10.7% more effective than the traditional rectangular baseline fin, while all other iterations were less effective than the baseline fin. However, the Sierpinski carpet fractal fins performed significantly better than the baseline iteration on a per unit mass basis after the first iteration. On average, the first, second, third, and fourth iterations were found to be approximately 1.1%, 7.5%, 26.4%, and 77.3% more effective per unit mass than the baseline fin. This trend was expected, as the mass of the Sierpinski carpet pattern fins decays exponentially with each fractal iteration, while the surface area available for heat transfer (which directly correlates to fin effectiveness) increases relative to the base fin after the third fractal iteration.

The fourth fractal iteration was found to be the best fractal fin design to promote increased passive thermal management, as it has a 23.3% decrease in mass relative to the baseline fin while simultaneously being more effective (10.7%) and more effective per unit mass (77.3%) and only slightly (10.2%) less efficient than the baseline fin.

When examining scalability of results between fractal fin sizes, the trends for these same fin performance metrics were studied from the previous research of Keten, who tested Sierpinski carpet pattern fins whose height, width, and thickness dimensions were twice as large as those studied in this investigation. His research produced similar results, with the efficiency steadily decreasing with each fractal iteration; however, the larger Sierpinski fractal fins experienced a larger decrease in efficiency of the fourth

iteration relative to the baseline iteration (approximately 15.5%) compared to the 10.2% drop in efficiency calculated for the small-scale Sierpinski carpet fractal fins in this experiment [5].

Additionally, identical trends were observed for the fin effectiveness and fin effectiveness per unit mass for each iteration relative to the baseline iteration, with the fourth iteration being found to be both more effective and more effective per unit mass than the baseline iteration. However, the fourth iteration small Sierpinski carpet pattern fractal fin in this study was found to be approximately 77.3% more effective per unit mass than the baseline case, whereas the fourth iteration of the larger Sierpinski carpet fractal fins studied by Keten were found to be only 66.4% more effective per unit mass than the baseline case. Notably, the small fractal fins were found to be roughly 8-9 times more effective per unit mass than their larger-scale counterparts [5]. This is likely due to the fact that the small-scale and large-scale fins had similar fin effectiveness values, while the small-scale fin iterations had approximately 12-13% of the mass of their large-scale counterparts. This suggests that the use of several small-scale fins rather than one large scale fin to dissipate waste heat from electronic systems would be more effectual in applications where maximizing effectiveness while reducing mass is essential.

Despite these discrepancies in percentage increases/decreases relative to the baseline fins, the overarching trends of decreasing efficiency with each iteration and increasing effectiveness per unit mass for each iteration were supported by the findings of both scales of Sierpinski carpet fractal fins.

In this study, the percentage of the heat dissipated via thermal radiation with respect to the total heat transfer of the system was taken into account as previous findings

from other researchers suggested that it was significant and should not be neglected. The results of this study support that hypothesis, as the percentage of heat transfer thermal radiation was found to be significant for all fractal iterations even after the calculated average fin view factor was applied to each fin. Between 33-42% of the total heat dissipated from the system was due to radiation, although with each increasing iteration, the average fin view factor decreases, meaning that more radiation is getting trapped inside the increasingly smaller perforations in the fin and engaging in inter-surface thermal radiation, causing less heat to radiate to the surroundings and contribute to the overall heat transfer of the system.

Future directions of study would include researching the fin performance of higher order fractal iterations; unfortunately, the cost of fabricating the higher order fractal iteration fins with any degree of accuracy is astronomically high and cost-prohibitive for most research purposes. This means that using the Sierpinski carpet fractal pattern fins in passive thermal management of electronic systems may be limited to applications where the cost benefits of reducing mass are considered compensatory for the increasing manufacturing complexity and associated higher cost thereof, such as in the aerospace industry, where mass reductions often result in astronomical savings. In future studies, attempts could be made to more accurately quantify the amount of heat lost through the insulation, though this amount was found to be less than 10% of the total heat transfer of the system for all iterations tested. In future studies, attempts should also be made to more accurately quantify the amount of heat dissipated by thermal radiation by conducting these tests in a vacuum environment, as this was found to be a significant contributor to the total heat transfer of the system (between 33-42%) and was also found

to be dependent on a variety of factors that affected the calculated average fin view factor. The inter-surface thermal radiation behavior of higher iteration fins could also be studied. The relationship between the percentages of heat dissipated due to thermal radiation and natural convection with respect to fractal iteration should be studied in the context of a view factor analysis, partially to study the effect of increasingly smaller fin perforations on the thermal radiation and natural convection behavior of the fins.

6. Conclusion

This experimental investigation sought to study the thermal performance of the first four iterations of the small-scale Sierpinski carpet pattern fins in a natural convection environment. While the fin efficiency decreased with each fractal iteration, the effectiveness per unit mass increased exponentially with each fractal iteration. The fourth fractal iteration fin was found to be the most promising fractal iteration in terms of fin performance, as it was found to be approximately 10.7% more effective and 77.3% more effective per unit mass than the baseline (zeroth iteration) fin while experiencing a 23.3% reduction in mass and only a 10.2% overall reduction in efficiency. However, the additional manufacturing cost of fabricating a small-scale Sierpinski carpet pattern fourth iteration fin is exceptionally high, and this might make the design only appealing in industries where the cost savings due to the reduced mass and simultaneous increase in effectiveness and effectiveness per unit mass would significantly offset the additional manufacturing costs, such as the aerospace industry for passive thermal management of electronic systems on spacecraft. Lastly, the results support previous findings that the contributions of thermal radiation to the system are significant (between 33-42%) and

dependent on fractal iteration and the corresponding average fin view factor, and therefore should not be neglected in future investigations.

References

[1] "Advanced Space Transportation Program: Paving the Highway to Space," National Aeronautics and Space Administration, [Online]. Available: https://www.nasa.gov/centers/marshall/news/background/facts/astp.html. [Accessed 29 March 2017].

[2] "Capabilities & Services," SpaceX, [Online]. Available: http://www.spacex.com/about/capabilities. [Accessed 29 March 2017].

[3] D. Calamas, D. Dannelley and G. Keten, "Experimental Effectiveness of Sierpinski Carpet Fractal Fins in a Natural Convection Environment," *Journal of Heat Transfer,* 2017.

[4] G. Keten, "Thesis: Thermal Performance of Sierpinski Carpet Fractal Fins in Natural and Forced Convection Environments," Georgia Southern University, Statesboro, 2016.

[5] D. Dannelley and J. Baker, "Natural Convection Heat Transfer from Fractal-Like Fins," *Journal of Thermophysics and Heat Transfer,* vol. 27, no. 4, pp. 692-699, 2013.

[6] D. Dannelley and J. Baker, "Natural Convection Fin Performance Using Fractal-Like Geometries," *Journal of Thermophysics and Heat Transfer,* vol. 26, no. 4, pp. 657-664, 2012.

[7] M. C. Coppens, "Scaling-Up and -Down in a Nature Inspired Way," *Industrial and Engineering Chemistry Research,* vol. 44, no. 14, pp. 5011-5019, 2005.

[8] D. Calamas and J. Baker, "Tree-Like Branching Fins: Performance and Natural Convective Heat Transfer Behavior," *International Journal of Heat and Mass Transfer,* vol. 62, pp. 350-361, 2013.

[9] H. Azarkish, S. M. Sarvari and A. Behzadmehr, "Optimum Geometry of a Longitudinal Fin with Volumetric Heat Generation under the Influences of Natural Convection and Radiation," *Journal of Energy Conversion and Management,* vol. 51, pp. 1938-1946, 2010.

[10] M. R. Shaeri and M. Yaghoubi, "Thermal Enhancement from Heat Sinks by Using Perforated Fins," *Journal of Energy Conversion and Management,* vol. 50, no. 5, pp. 1264-1270, 2009.

[11] M. R. Shaeri, M. Yaghoubi and K. Jafarpur, "Heat Transfer Analysis of Lateral Perforated Fin Heat Sinks," *Journal of Applied Energy,* vol. 86, pp. 2019-2029, 2009.

[12] M. R. Shaeri and T. C. Jen, "The Effects of Perforation Sizes on Laminar Heat Transfer Characteristics of an Array of Perforated Fins," *Journal of Energy Conversion and Management,* vol. 64, pp. 328-334, 2012.

[13] S. H. Yu, D. Jang and K. S. Lee, "Effect of Radiation in a Radial Heat Sink Under Natural Convection," *International Journal of Heat and Mass Transfer,* vol. 55, pp. 505-509, 2012.

[14] D. Dannelley and J. Baker, "Radiant Fin Performance Using Fractal-Like Geometries," *Journal of Heat Transfer,* vol. 135, no. 8, 2013.

[15] A. J. Wheeler and A. R. Ghanji, Introduction to Engineering Experimentation, 2nd ed., Upper Saddle River: Prentice-Hall, 2003.